# 50-500 GHz Wireless: Transistors, ICs, and System Design

M. J. W. Rodwell

Department of Electrical Engineering University of California, Santa Barbara, CA 93105

*Abstract* —**50–500 GHz phased-array transmitters and receivers have high available bandwidth, can support multiple independent spatial transmission channels, but suffer from extremely high worst-case foul-weather attenuation. Link analysis suggests that several useful systems can be realizing using power amplifiers with ~50-200 mW output power, low-noise amplifiers with ~4-7 dB noise figure, and arrays of ~64-128 elements. Such systems can be realized with Si VLSI beamformers, InP HEMT low-noise amplifiers (LNAs), and InP HBT or GaN HEMT power amplifiers (PAs). Scaling analysis of present InP HBTs and HEMTs suggests that their power-gain cutoff frequencies can be extended from the present ~1.2-1.4 THz to at least 2-3 THz, thereby supporting high-performance PAs and LNAs for such systems even at 500 GHz.**

**Index Terms — wireless ICs, bipolar transistors, mm-waves, sub-mm-waves, THz.**

## I. Introduction

With progressive scaling, meaning reduced lithographic dimensions, reduced semiconductor and dielectric layer thicknesses, increased current densities and reduced contact resistivities, transistor bandwidths continue to increase. InP HBTs have attained over 1 THz $f_{max}$ [1,2,3] and >600 GHz ICs [4] have been demonstrated with this technology. InP HEMTs have also attained $f_{max}$ significantly above 1 THz, and, with these, 650 GHz amplifiers [5] have been reported. Even in (32 nm SOI) CMOS VLSI [6], with its more limited transistor cutoff frequencies but vastly greater feasible integration scales, transceivers operating in fundamental mode have been demonstrated at 210GHz.

Demonstrated transmitter output power is strongly dependent both on device technology and upon frequency; Monolithic power amplifier (PA) results include ~2W at 94 GHz [7] from GaN HEMTs, 180 mW at 180 GHz [8] and 1.9 mW at 600GHz [4] from InP HBTs, 102mW at 62 GHz [9] and 10mW at 160 GHz [10] from SiGe HBTs, and 17mW at 80 GHz [11] and 2.9mW at 201 GHz [6] from Si CMOS. Harmonic generation in any of these technologies extends the feasible frequency range, albeit at a high cost in both output power and efficiency. Receiver noise figure similarly varies strongly with frequency and with choice of technology; receiver harmonic mixing techniques (with the LNA omitted) increase frequency range at the expense of sensitivity. To select among these technologies in developing future 50-500GHz systems, we must consider system design. We suggest that outdoor systems in these bands will use moderately large phased arrays with CMOS signal processing, InP HBT or GaN HEMT power amplifiers, and InP HEMT low-noise amplifiers.

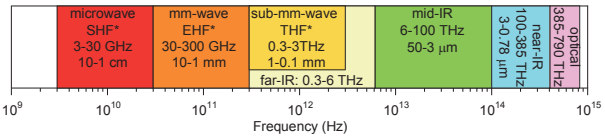


Figure 1: The electromagnetic spectrum from microwave to the visible. Bands* per ITU standard; IR bands per ISO 20473.

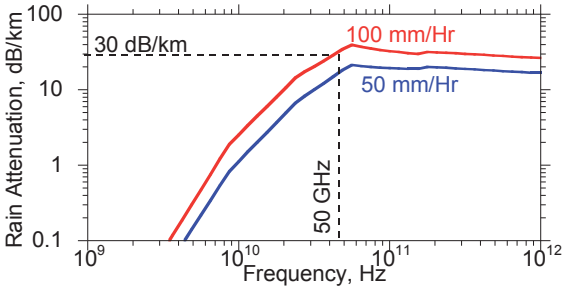


Figure 2: Rain attenuation at 50 mm/hr and 100 mm/hr (exceeded at $10^{-5}$ probability), calculated from ref. [8]

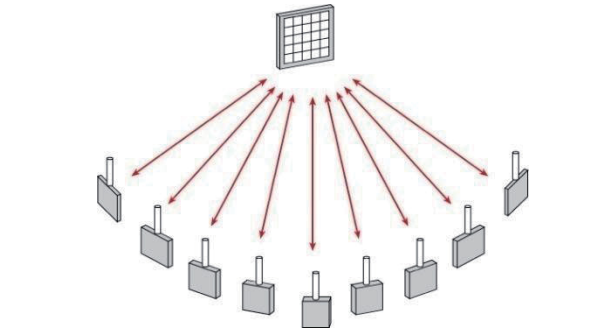

(a)

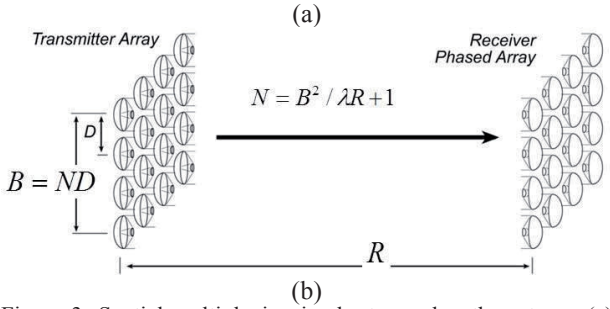


(b)

Figure 3: Spatial multiplexing in short-wavelength systems. (a) Phased-array beam steering in a network base station for multiple independent beams at a given carrier frequency. (b) Spatial multiplexing in a line-of-sight mm-wave MIMO link, with the capacity varying as the inverse square of wavelength.

ISBN 978-3-8007-3585-3

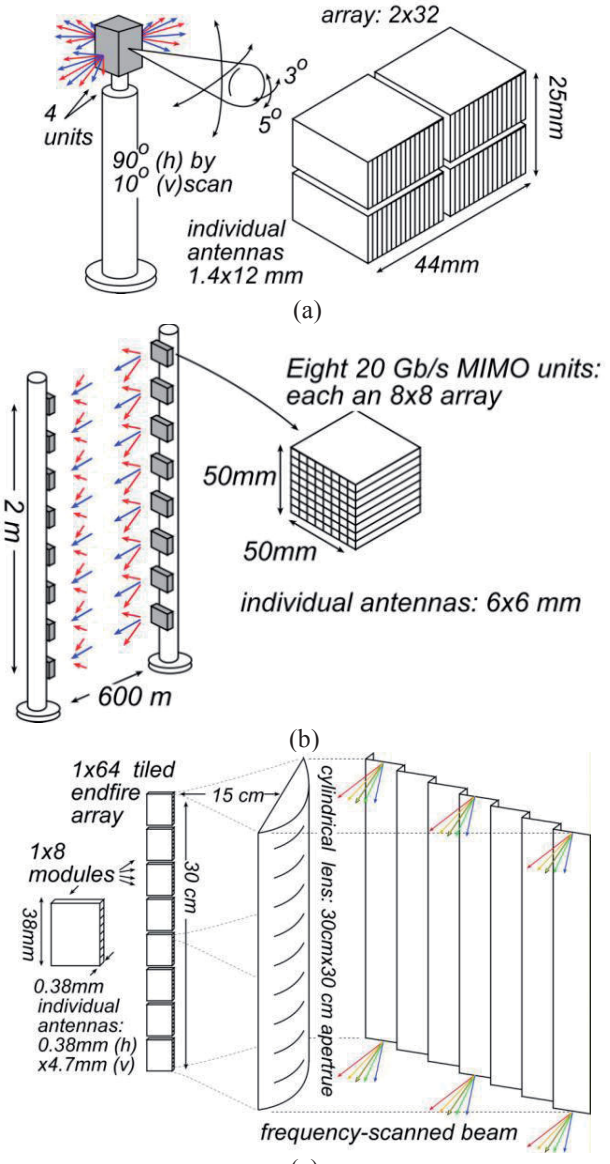


Figure 4: Example mm-wave and sub-mm-wave systems. (a) A 140 GHz, 10 Gb/s adaptive picocell backhaul unit using 64-element arrays . (b) A 340 GHz, 8-channel 160 Gb/s MIMO backhaul link, using 64-element subarray transceivers. (c) A 400 GHz frequency-scanned imaging car radar providing 64x512 elements.

## II. MM-WAVE/SUB-MM-WAVE SYSTEMS

Sub-mm-wave and mm-wave (Figure 1) wireless systems can provide very high data capacity. In clear weather, there are large bandwidths at 75-110, 125-165, and 200-300 GHz between absorbtion lines, and narrower bands at higher frequencies. The short wavelengths allow many parallel spatial channels. Phased array base stations (Figure 1a) can provide multiple beams with an angular resolution proportional to $\lambda/(\text{array width})$. Line-of-sight MIMO links (Figure 1b) provide capacity proportional to $1/\lambda^2$ [12]. Unfortunately, propagation loss is high, both from $\lambda^2/R^2$ propagation losses and from foul-weather attenuation. Under 5-9's conditions, rain attenuation [13] is ~30 dB/km from 50-1000GHz, dominating over fog [14] below ~500GHz; 50-500 GHz links must tolerate ~30 dB/km attenuation. Further, the area $\sim \lambda R$ of the first Fresnel zone is small, hence beams are easily blocked. Phased array transceivers are desirable both for adequate transmission range (small-beamwidth, fix-aimed antennas are expensive to install) and to provide *adaptive beam steering* in *mesh networks* to accommodate beam blockage.

## II. SYSTEMS EXAMPLES

Consider three example systems (Figure 4). The first is a 140 GHz, 10 Gb/s picocell backhaul unit using 64-element arrays. In the event of beam blockage, the arrays steer the transmission to an alternate network node. Given realistic packaging loss, operating & design margins*, power amplifiers (PAs) with $P_{sat} = 24$ dBm per array element, and low-noise amplifiers (LNAs) with $F$ =4 dB, the units can operate over 350 m range (almost two city blocks) in 5-9's rain.

The second is a 340 GHz, 160 Gb/s MIMO backhaul link. This employs a linear 1x8 MIMO superarray, with each element comprised of a 64-element subarray module. Here, given PAs having 24 dbm $P_{sat}$ per element, and LNAs having $F$ =4 dB, range† in 5-9's rain is 600 meters.

The third is a heads-up-display 400 GHz automotive imaging radar, using a linear 1x64 array and frequency-scanned beam steering with a 30cm$^2$ lens and diffraction grating to form a TV-like picture with 60-Hz-rate, 64x512 pixels, 0.14° resolution, and 10dB-SNR image from a 1 ft$^2$ target at 300m range in heavy fog. Necessary peak output power is 50mW/element given 6.5dB LNA noise figure‡.

For these examples, low receiver noise figure and high transmitter output power are necessary for the desired system transmission range. Noting that today's cellular telephones use III-V PAs and LNAs, we suggest that such systems are best realized (Figure 5) with a combination of Si VLSI beam steering ICs and III-V (GaN or InP) PAs and LNAs. ICs can be assembled into phased arrays using Si MEMS wafer-level packaging [15, 16].

In CMOS (sub) mm-wave systems [6], PA output power is lower and LNA noise figure higher than that achievable with III-V technologies. In this case, the necessary system

* Analysis: Propagation loss from the Friis transmission equation, sensitivity from symbol rate assuming lightly-coded QPSK, array directivities from areas. 6dB package loss, 3dB end-of-life, 6dB design margin, 10dB operating margin, 5dB obstruction loss, 5dB PA backoff..

† Analysis: 1° beam width, 8° beam steering, lightly-coded 16QAM, loss & margins similar to example (a).

‡ Analysis: radar range equation, 10dB package loss, 5dB end-of-life, 2% pulse duty cycle, fog @34dB/km.

ISBN 978-3-8007-3585-3

range can be obtained by increasing the number of transmitter and receiver array elements while maintaining a fixed area each individual element. As the array size increases, directivities increase and both the required per-element transmitter output power and the total required radiated power deceases. Because power is consumed in signal distribution and phase-shifting, there is an intermediate, optimum array size which minimizes power consumption. Figure 6 shows *example* calculations for the array of Figure 4a, where it is found that a ~128-element array provides best power efficiency. Low-power phase-shifters and low-power signal distribution are necessary if large arrays are to be viable.

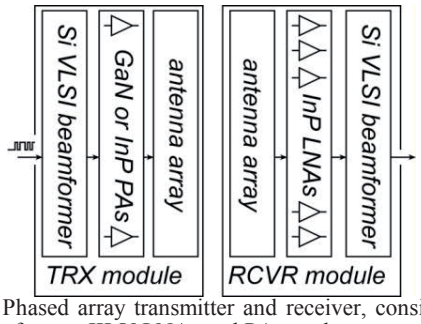


Figure 5: Phased array transmitter and receiver, consisting of a VLSI beamformer, III-V LNAs and PAs, and antenna array.

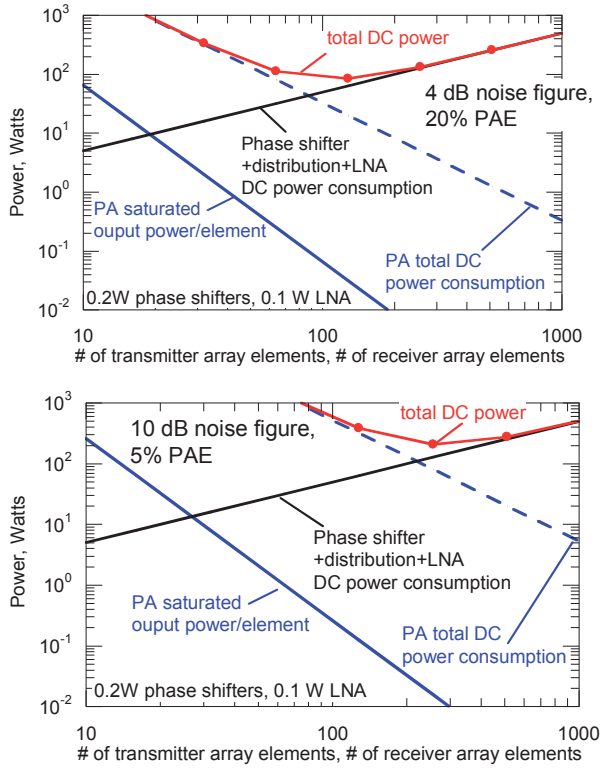


Figure 6: Computed transmitter and receiver power consumption as a function of array size for the system of fig. 4a. As array size increases, required power per PA decreases but power consumed in the beam steering and signal distribution increases.

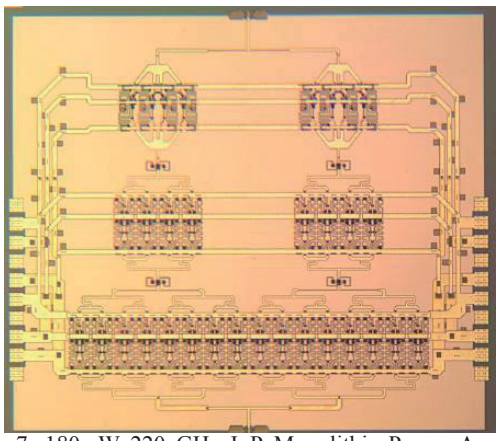

Figure 7: 180mW 220 GHz InP Monolithic Power Amplifier. The die is 2.51x2.22mm$^2$.

## Transistor and IC results.

Work at UCSB has focused on both THz transistor and mm-wave IC development. We will present results on THz InP HBT development at the 130 nm node, and on power amplifiers at 85GHz and 220 GHz [8] (Figure 7).

## Acknowledgment

Portions of this work were performed in the UCSB Nanofabrication Facility, a member of the NSF-funded National Nanofabrication Infrastructure Network. Program support by the DARPA THETA, Hi-Five, and Hotspots programs is acknowledged.

## Reference

[1] M. Urteaga, R. Pierson, P. Rowell, V. Jain, E. Lobisser, M.J.W. Rodwell, 2011 IEEE Device Research Conference, June 20-22, Santa Barbara.

[2] V. Jain, J. C. Rode, H-W. Chiang, A. Baraskar, E. Lobisser, B. J. Thibeault, M. Rodwell, M. Urteaga, D. Loubychev, A. Snyder, Y. Wu, J. M. Fastenau, W.K. Liu, 2011 IEEE Device Research Conference, June 20-22, Santa Barbara.

[3] M. J. W. Rodwell, J. Rode, H.W. Chiang, P. Choudhary, T. Reed, E. Bloch, S. Danesgar, H-C Park, A. C. Gossard, B. J. Thibeault, W. Mitchell, M. Urteaga, Z. Griffith, J. Hacker, M. Seo, B. Brar, IEEE Compound Semiconductor Integrated Circuit Symposium (CSICS), 2012 IEEE, San Diego, Oct. 2012.

[4] M. Seo, M. Urteaga, J. Hacker, A.Young, A. Skalare, R. Lin, M. Rodwell, 2013 International Microwave Symposium, 2-7 June, Seattle.

[5] V. Radisic, K.M.K.H. Leong, X. Mei, S. Sarkozy, W. Yoshida. W.R. Deal, IEEE Trans MTT vol.60, no.3, pp.724,729, March 2012.

[6] Z. Wang, P.Y. Chiang, P. Nazari, C.-C. Wang, Z. Chen, and P. Heydari, IEEE Int'l Solid-State Circuits Conference (ISSCC), Feb. 2013.

[7] M. Micovic, A. Kurdoghlian, A. Margomenos, D.F. Brown, K. Shinohara, S. Burnham, I. Milosavljevic, R. Bowen, A.J. Williams, P. Hashimoto, R. Grabar, C. Butler, A. Schmitz, P.J.

ISBN 978-3-8007-3585-3

Willadsen, and D.H. Chow, 2012 IEEE IMS, pp.1,3, 17-22 June 2012.
[8] T. B. Reed, Z. Griffith, P. Rowell, M. Field, M. Rodwell, 2013 IEEE Compound Semiconductor IC Symposium, October 13-16, Monterey, California.
[9] Z. Yi, J.R. Long, IEEE Journal Solid-State Circuits, vol.47, no.9, pp.1981-1997, Sept. 2012.
[10] N. Sarmah, P. Chevalier, and U. Pfeiffer, IEEE Transactions on Microwave Theory and Techniques, vol. 61, no. 2, pp. 939–947, February 2012 .
[11] J. Kim, H. Dabag, P. Asbeck, J. F. Buckwalter, IEEE Transactions on Microwave Theory and Techniques, vol.60, no.6, pp.1870,1877, June 2012.
[12] E. Torkildson, U. Madhow, M. Rodwell, IEEE Trans. Wireless Comms., vol.10, no.12, pp.4150-4160, December 2011.
[13] R. Olsen, D. Rogers, D. Hodge, IEEE Trans. Antennas and Propagation, vol.26, no.2, pp. 318- 329, Mar 1978.
[14] H.J Liebe, T. Manabe, G.A. Hufford, IEEE Transactions on Antennas and Propagation, Volume 37, Issue: 12 , Dec. 1989.
[15] I. Mehdi, G. Chattopadhyay, Choonsup Lee, T. Reck, C. Jung, J. Siles, K. Cooper, N. Llombart, 7th European Microwave Integrated Circuits Conference (EuMIC), pp.230-233, 29-30 Oct. 2012.
[16] K.M.K.H. Leong, K. Hennig, C. Zhang; R.N. Elmadjian, Z. Zhou, B.S. Gorospe, P.P. Chang-Chien, V. Radisic, W.R. Deal, EEE Transactions on Microwave Theory and Techniques, vol.60, no.4, pp.998,1005, April 2012.

ISBN 978-3-8007-3585-3